Crosstalk-Compensated Optical Phased Arrays for Wide-Angle Beam-Steering

Ankita Sharma[1,2,*], John N. Straguzzi[1], Tianyuan Xue[1,2], Alperen Govdeli[1,2], Fu-Der Chen[1,2], Andrei Stalmashonak[1], Wesley D. Sacher[1], and Joyce K.S. Poon[1,2]
[1]*Max Planck Institute of Microstructure Physics, Weinberg 2, 06120 Halle (Saale), Germany*
[2]*Department of Electrical and Computer Engineering, University of Toronto, 10 King's College Rd., Toronto, Ontario M5S 3G4, Canada*
**ank.sharma@mail.utoronto.ca*

Abstract: We demonstrate beam-steering over ~115° using independent amplitude and phase control to compensate for optical crosstalk in an optical phased array with 1mm-long waveguide grating emitters spaced at a ~λ/2 (775 nm) pitch.

1. Introduction

Optical Phased Arrays (OPAs) have gained considerable attention as compact beam-scanners with the capability for high-resolution beam-forming. They find key applications in Light Detection and Ranging (LiDAR) systems and free-space optical communications [1]. The ideal configuration for effective beam-forming requires that the light emitters, commonly implemented as long weak gratings, are spaced at intervals of less than λ/2. This configuration minimizes the sidelobes, thereby increasing the steering range of the optical beam. However, such close spacing introduces a significant challenge: optical crosstalk between adjacent emitters.

Previous efforts to mitigate this issue have focused on aperiodic grating pitch to reduce sidelobe levels by redirecting the power carried in higher order grating lobes [2]. While effective to some extent, this method has the trade-off of reducing the power carried in the main lobe, which is not desirable for applications requiring high-power, directed beams. Other efforts based on edge-emitting arrays have achieved half-wavelength spacing, by introducing a phase mismatch between neighboring edge emitting waveguides. However, these OPAs are limited to one-dimensional (1D) steering [3]. Adopting a similar approach for two-dimensional (2D) beam steering with detuned neighboring grating antennas is not as straightforward [4].

In this work, we introduce a novel approach to compensate for the crosstalk in OPAs commonly used for 2D beam-steering. Our method involves amplitude and phase correction of each individual grating antenna element. The grating antennas in our design are 1mm-long and spaced at a pitch of 775nm, satisfying the λ/2 criterion for minimal sidelobes, while maintaining a large effective aperture length in the grating axis of the phased array. Using our approach, a wide scanning range of 115° was measured. In this range, the highest measured sidelobe suppression was 14.5 dB, which was achieved without significantly compromising the power of the main lobe.

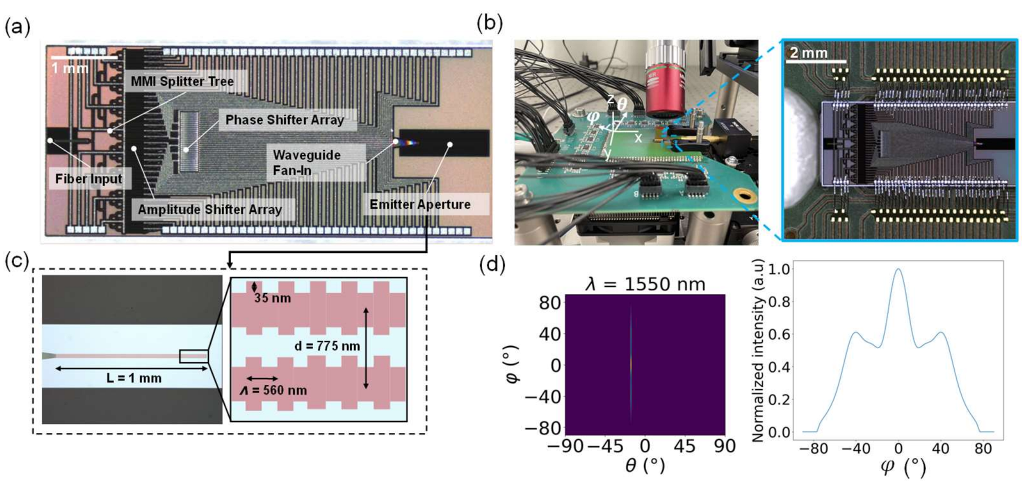

Fig. 1. (a) Annotated micrograph of the OPA chip. (b) Electrically packaged OPA with inset showing wire-bonded device. The beam can be steered in the angles θ and φ. (c) Micrograph and diagram of the emitting aperture. (d) Simulated far-field emission pattern of a single grating and line-cut along the φ-axis showing the emitting profile.

2. Operation Principle

To model the crosstalk, we consider a multi-input multi-output system, which relates the input to the OPA, represented as a complex vector of field amplitudes, $\vec{a}_{in} = [a_1, a_2 \ldots, a_N]$, to the complex field outputs,

$\vec{b}_{out} = [b_1, b_2 \ldots, b_N]$. $\vec{b}_{out}$ is related to $\vec{a}_{in}$ through the N × N transfer matrix, C, representing the coupling between elements in the array. While $\vec{b}_{out}$ can be generally defined, to form a single beam at a particular angle, $\vec{b}_{out}$ should be of the form $\vec{b}_{out} = [\alpha_1, \alpha_2 e^{i\Delta\phi} \ldots, \alpha_N e^{iN\Delta\phi}]$, where $\{\alpha_i\} \in \mathbb{R}$. Thus, we can determine a suitable input that would result in this output. The input amplitude and phases would compensate for the crosstalk if they are related to $\vec{b}_{out}$ as follows,

$$\vec{a}_{in} = C^{-1}\vec{b}_{out} \quad (1)$$

Since the elements in C and $\{\alpha_i\}$ are not fully known *a priori,* compensating for the crosstalk in the array becomes an optimization problem to realize $\vec{a}_{in}$ for different values of $\Delta\phi$. In practice, the values of α_i that form $\vec{a}_{in}$ can be found through optimization of the amplitude and phase of each element in the OPA through an algorithm such as the genetic algorithm. Assuming there are no amplifiers, we can choose to normalize $\vec{b}_{out}$ in Eq.(1) such that $|\alpha_i| \leq 1$.

2. Photonic Circuit Design

To validate this approach, we designed a 1×32-element OPA with independent amplitude and phase control of each grating antenna. 2D beam-steering is possible through a combination of wavelength and phase tuning. The photonic circuit, annotated in Fig. 1(a), was fabricated in the CMC Microsystems active silicon (Si) photonics multi-project wafer run at Advanced Micro Foundry. The circuit consisted of 64 active titanium nitride heaters; two in each channel to control amplitude and phase using the thermo-optic effect. For amplitude modulation we used a balanced Mach-Zehnder interferometer (MZI) with one output of the MZI terminating in a "dump" port. The heaters were wire-bonded to a printed circuit board and controlled via a high frequency pulse width modulation (PWM) controller from a field-programmable gate array (FPGA). The PWM generator was implemented using two separate frequency counters to achieve a > 8-bit resolution at a given repetition rate, as described in [5]. Figure 1(b) shows the packaged OPA on a custom printed circuit board mounted on a thermoelectric cooler.

To restrict the inter-waveguide coupling to the grating antenna region, the widths of the waveguides were varied periodically in the fan-in section leading to the emitter aperture. A schematic of the waveguide grating antennas in the emitter aperture is shown in the inset of Fig. 1(a). We used 1mm-long weak waveguide grating antennas with a grating period of 560nm and a 35nm corrugation width to create a low-divergence beam in the θ-axis. The pitch between grating antennas in the array was 775nm, near ~λ/2 criterion. The simulated 3D FDTD far-field emission pattern of a single grating at wavelength of 1550nm is shown in Fig. 1(c), as well as a vertical-line cut of the simulation in the φ-axis highlighting the emitting profile of the grating. The full-width half maximum (FWHM) of the emitting profile is ~100°, which limits the steering range of our OPA device. In the future, the single waveguide grating antenna design can be optimized for broader emission in φ [2].

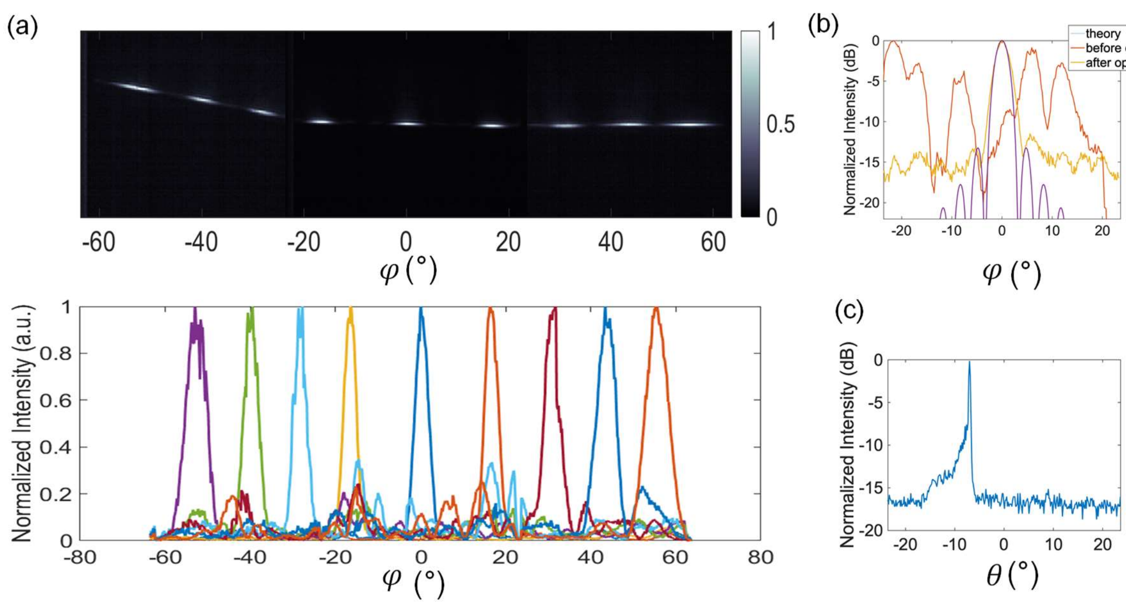

Fig. 2. (a) Top: Superimposed measured far-field images of beam steering in φ after optimization. Bottom: Elliptical cross-sectional cuts of the far-field emission above. (b) Comparison of cross section of beam solution at zero degrees with the diffraction pattern of a uniformly illuminated rectangular aperture. (c) Vertical line-cut of zero-degree solution in the θ-axis.

4. Experimental Results

To characterize the performance of our OPA, we rotated a Fourier imaging system that had a ~47° field-of-view (FOV). Images were captured with the imaging system tilted at different angles in φ and stitched together to measure a wider FOV. A multi-objective genetic algorithm was used to find an initial solution of Eq. (1) for $\Delta\phi = 0$, by maximizing both the signal to noise ratio and integrated power in a region of interest surrounding a beam centered at φ =0° [6]. Once a single beam was formed in the far-field at a specified angle we knew that we had optimized $\vec{a}_{in}$ to find $\vec{b}_{out}$ of the form $\vec{b}_{out} = [\alpha_1, \alpha_2 e^{i\Delta\phi} \ldots, \alpha_N e^{iN\Delta\phi}]$. Subsequent solutions of $\vec{a}_{in}$ for different values of $\Delta\phi$, and φ were found using the pattern search algorithm to reduce the optimization search space. Figure 2(a) shows the beam formed at nine different angles in φ at a constant wavelength of λ = 1450nm. This wavelength was selected because it resulted in near-normal emission (~θ =-5°), such that the Fourier imaging system could be rotated along φ while remaining fixed at θ = 0°. However, given that small rotations of the imaging system in the θ-axis were unavoidable, the cross-sectional cuts in Fig. 2(b) are taken along an elliptical arc to account for rotations in θ as described in [7]. Figure 2(c) compares the optimized solution at φ = 0° to the theoretical sinc^2 diffraction pattern of a uniformly illuminated rectangular aperture with 32 emitters at a pitch of 0.775 um. The two beam profiles show a high degree of similarity demonstrating successful control over the crosstalk in the emitting aperture. To extend this work to 2D beam-steering, the optimization process can be repeated for different wavelengths.

Further analysis of the key performance metrics of the OPA beam profiles in Fig. 2 are illustrated in Fig. 3. The sidelobe levels we report in Fig.3(a) are a measure of the maximum intensity in the main lobe to the maximum peak intensity outside the lobe in a 2D region defined by, $[\theta_{min}, \theta_{max}] = [-23.6°, 23.6°]$ and $[\varphi_{min}, \varphi_{max}] = [-63.6°, 63.6°]$. The power in the main lobe is the integrated pixel power in the direction of the beam between first nulls divided by the total pixel power in the aforementioned 2D region. The best optimized solution had a sidelobe level of 14.5 dB and more than 50% of the total emitted power in the main lobe. This is 10% more power than the theoretical maximum of an optical phased array with 192 waveguides and an optimized random aperiodic pitch [4]. The beam widths shown in Figure 3(b), which were ~3.5°, were limited by the aperture size of the array.

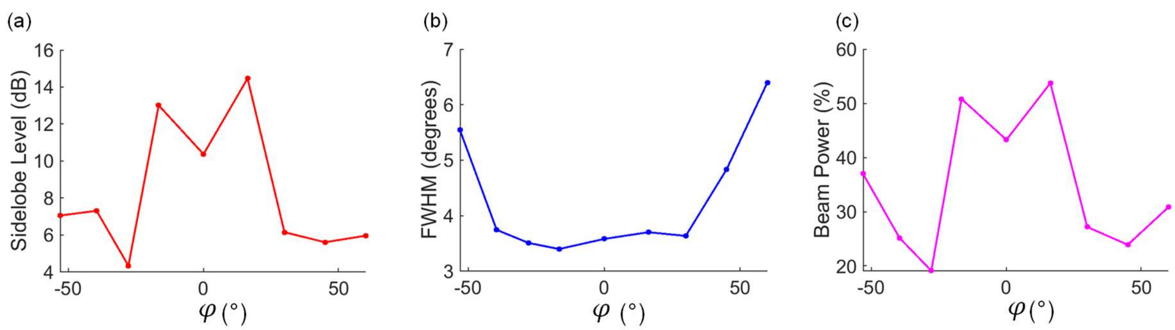

Fig. 3. For various angles in *φ:* (a) Measured Sidelobe level of the beam. (b) Measured FWHM of the beam (c) Power in beam as a percentage of total radiated power.

5. Conclusion

In summary, we have experimentally demonstrated optical crosstalk compensation in an 1x32-element optical phased array using amplitude and phased control. The phased array circuit had 1mm-long waveguide grating antennas placed at an approximately half-wavelength pitch. We characterized the circuit at λ = 1450 nm and validated its performance over a field of view of 115°. The compensation technique presented here is versatile and applicable to various applications where there is a need for densely packed, uniform arrays of waveguides or gratings with minimal crosstalk.

6. References

[1] C. V. Poulton *et al.,* "Long-Range LiDAR and Free-Space Data Communication with High-Performance Optical Phased Arrays," IEEE J. of Sel. Top. Quantum Electron. **25,** 7700108, (2019).
[2] Y. Li et al., "Wide-steering-angle high-resolution optical phased array," Photon. Res. **9**, 2511-2518 (2021).
[3] C. T. Phare, et al., "Silicon Optical Phased Array with Grating Lobe-Free Beam Formation Over 180 Degree Field of View," Proc. CLEO, 2018, paper SM3I.2.
[4] T. Komljenovic et al "Sparse aperiodic arrays for optical beam forming and LIDAR," Opt. Express **25**, 2511-2528 (2017).
[5] H. Matsuura, et al. "Accelerating Switching Speed of Thermo-optic MZI Silicon-Photonic Switches with "Turbo Pulse" in PWM Control," *Proc. OFC*, 2017, paper W4E.3.
[6] Q. Liu *et al*., "Silicon Optical Phased Array Side Lobe Suppression Based on an Improved Genetic Algorithm," *Proc. ACP and IPOC (*2020), pp. 1-3.
[7] D. N. Hutchison et al., "High-resolution aliasing-free optical beam steering," Optica **3**, 887-890 (2016).